Dichotomy in Growth and Invasion From Low to High Grade Glioma Cellular Variants

Krishnendu Ghosh
Panihati Mahavidyalaya and University of Calcutta
Samarandranath Ghosh
Institute of Postgraduate Medical Education and Research Bangur Institute of Neurology
Uttara Chatterjee
Institute of Postgraduate Medical Education and Research
Pritha Bhattacharjee
University of Calcutta
Anirban Ghosh (aghosh06@gmail.com)
Netaji Subhas Open University https://orcid.org/0000-0001-7349-2622

Research Article

Keywords: Glioma, Proliferation, Invasion, Angiogenesis, GAM, Dichotomy

Posted Date: March 1st, 2021

DOI: https://doi.org/10.21203/rs.3.rs-265328/v1

Abstract

Glial dysfunction outraging CNS plasticity and integrity results into one of the most dangerous cancer, namely glioma, featuring little median survival period and high recurrence. The hallmark properties of proliferation, invasion and angiogenesis with the infiltrated macrophages in glioma are expected to be tightly coupled or cross-linked, but not definitely related so far. Present study is aimed to find a relationship between this featured quadrangle from lower to higher grades of post-operative glioma tissues and their invading subsets. Elevated Ki67 associated proliferation in lower grades was supported with VEGF dependent angiogenic maintenance which found decrease unlikely in higher grades. In contrast, MMP-2 and 9 associated invasions augmented high in higher grades with dominant presence of $CD204^{+}$ M2 polarized macrophages and a general increase in global DNMT1 associated methylation. Marked differences found in ECM invading cellular subsets of higher grades showing high proliferative capacity indicating rationally for recurrence, contrasting the nature of gross tumor tissue of same grade. Thus in lower grades the neoplastic lesion is more inclined for its growth while in higher grade more disposed towards tissue wreckage in support with cellular environmental milieu whereas the cellular variants and subsets of invaded cells showed different trends. Therefore, some operational dichotomy or coupling among cellular variants in glioma is active in determining its low to high grade transition and aggressive progression.

Introduction

Glioma, the cancer of glial cells, are the most common type of primary intracranial neoplastic lesion, representing majority of brain tumor malignancies with minimal prognostic efficiency. Due to high invasiveness they show poor prognosis, making the medial survival of 12-15 months post-detection [Ostrom et. al., 2014]. If the fundamental features of a neoplastic growth is analyzed, it has been found that several features like sustaining proliferation, resisting cell death, replicative immortality etc. are connected with tumor growth property and others like invasion, metastasis and angiogenesis are basically related to its motility or spreading [Hanahan and Weinberg, 2011]. Basically, proliferative and viability circuit of cancer coupled with its motility vigor determines the deadliness of any neoplasm, and present evidences are pointing the crucial roles of tumor microenvironment as well as inflammatory involvement in moulding the aggressive nature of any cancer [Gajewski et. al., 2013; Stuelten et. al., 2018; Nallanthighal et. al., 2019]. Glioma, being one of the deadliest among the neoplastic spectrum, possesses high invasiveness propelled with immune-inflammatory association along with its higher proliferation [Friedmann-Morvinski, 2014; Ghosh et al, 2017]. In course of gliomagenesis, the neoplastic cells proliferate randomly and rapidly, that is i.e., ‘Grow’, while reinforcing with nutrition and gaseous supply by neo-angiogenesis and simultaneously invade to re-colonize at newer areas as ‘Go’ by degrading surrounding tissues, basement membrane of blood vessels and myelinated nerve fibers [Rao, 2003; Louis, 2006]. Thus glioma progression can be restructured into two vectors: the ‘Go’ and ‘Grow’. Hypothesis suggests highly migrating glioma cells show lesser proliferative nature and *vice versa* giving birth to the “Go versus Grow dichotomy” [Giese et al, 2003; Saut et al, 2014].

In Glioma, matrix metalloproteinases (MMPs), different serine/cysteine proteases have important contribution for invading the surrounding tissue. Among them MMP-2 and MMP-9 are categorized as gelatenase, which are reported to have prominent roles with increasing glioma grades and directly correlated with cell migration and invasion [Wild-Bode et al, 2001; Ramachandran et al, 2017]. In contrast to this phenomena of invasion or 'Go', the 'Grow' or proliferation has been widely identified with Ki67 which in some cases reported to increase with glioma grading, but few contradicting observations showed its over-expression in grade II or lower grades [Yuan et al, 2013; Ramachandran et al, 2017; Xue et al, 2017;]. Such two basic features are perceptibly coupled with angiogenesis and intrusion of macrophages at glioma site and inflammation [Hanahan and Weinberg, 2011; Murat et al, 2009; Matias et al, 2018].It is also found that the magnitude of macrophage presence and glioma grades are positively correlated which have shown possible involvement of M2 macrophages/microglia [Komohara et al, 2008; Gieryng et al, 2017]. So the heterogeneity of glioma microenvironment, though complexly regulated by different stakeholders, has been divided into two fundamental driving urges of the neoplastic tissue i.e., 'grow' and 'go' with associated angiogenic support and with obvious neighborhood of glioma associated microglia/macrophage (GAM) population. The interrelation of mentioned featured quadrangle had been investigated to detect whether such dichotomy does actually exists in real patient glioma samples or balanced in some other ways.

The phenomena in low and high grade of astrocytoma with post-operative human glioma tissue samples had been tried to characterize over both the both over the whole tissue, surviving cells in culture and isolated cells passing through mimicked Extracellular Matrix (ECM) condition as invading subtypes. Moreover association of angiogenic property, brain macrophage/microglia and their polarization status along with incurring epigenetical changes in terms of global methylation have also been compared from lower to higher grade transition of glioma. Present investigation is aimed to find a relationship between the featured quadrangle of proliferation-invasion-angiogenesis-inflammation by studying characteristic marker expression at different levels from lower to higher grades of post-operative glioma tissues and their invading subsets. Such holistic approach on these basic features of glioma brought probably would probably bring a newer insight on glioma progression in patients which may open up some better prognostic approaches.

Materials And Methods

Patient Samples and Grading:

The post-operative crude neoplastic tissue fractions were collected from Bangur Institute of Neurosciences, Institute of Post Graduate Medical Education and Research (IPGME&R), Kolkata, India as per institutional ethical clearance (vide Memo No. Inst/IEC/553 dated 15.01.2014) after the neuro-oncosurgery surgery and fixed in selective mediums as per methodological requirements. Relevant clinical details and data of Magnetic Resonance Imaging (MRI) done with 1.5 Tesla multi-sliced MR imager with whilst T1 & T2 weighted contrast enhanced parameters along with MR spectroscopy values on choline/creatine ratio, N-acetylaspertate (NAA) and lactate peaks had been collected. All glioma

samples were primarily of adult, pediatric and recurring types from which only the adult non-recurring glioma tissues of six (n=6) low grade [i.e, astrocytoma grade II] and five (n=5) high grade [i.e, anaplastic astrocytoma or grade III and glioblastoma multiforme or GBM or grade IV] samples were included in the study. The pathological grading of post-operative tissues were done by collaborating histopathology department of IPGME&R according to WHO 2007 and 2016 protocol. All the parameters were performed for all samples unless otherwise mentioned in figure legends. Therefore, in low grade n=6 and in high grade n=5. All experiments had been done at least in duplicate.

Tissue Immunohistochemistry with Hematoxylin Counter-staining

Tissues fixed in 4% para-formaldehyde embedded in paraffin blocks were processed as 10 µm thick tissue ribbons and fixed in glass slides. De-paraffinized, gradually hydrated with descending alcohol grades, phosphate buffer Saline (PBS) washed and blocked by 3% Bovine Serum Albumin (BSA) solution (LOBA Chemie, India) for 30 minutes followed by overnight incubation of primary non-conjugated human reactive rabbit monoclonal anti-Ki67 (Santacruz Biotechnology, Dallas, TX, USA) overnight at 4^0C moist chamber. Slides washed in PBS were treated with Horse Raddish Peroxidase (HRP)-conjugated rabbit reactive mouse secondary antibody (Santacruz Biotechnology, Dallas, TX, USA), treated with 3,3-diaminobenzidine (DAB) (SRL, India) in buffered (1M TRIS, p^H 7.4) hydrogen peroxide solution along with 0.5% copper sulfate solution in dark followed by counter-staining with Dellafield's hematoxylin solution (Merck, India) and dehydrated in alcohol to reach in air dried condition. Similar protocol was administered in detecting total methylation pattern in tissue level among high and low grade of astrocytomas using human reactive rabbit monoclonal DNA Methyl Transferase 1 (DNMT1) with HRP conjugated mouse anti rabbit secondary antibody (both from Santacruz Biotechnology, Dallas, TX, USA). Both the primary antibodies were added at 1:200 dilution and secondary added 1:500 dilution in 1% BSA solution. These slides mounted with DPX, were visualized in bright field under Nikon Microscope (TS 100-F Eclipse, Nikon Corp., Japan), photographed with CCD Camera (DS-Fi2-U3) and analyzed with NIS Element-BR Software (Nikon Corp., Japan) for mitotic activity and epigenetic methylation attributes associated with these tumor types. In both the cases photographs were being evaluated as their expression profiling using 'Fiji_ImageJ2 software' (NIH, USA).

Tissue Immunohistochemistry with Fluorescence Microscopy

Tissue samples fixed in glass slides as mentioned earlier and after overnight hit fixation, all samples were stained separately with – (1) primary non-conjugated human reactive mouse monoclonal anti-matrix metalloproteinase 2 (MMP2) antibody (Novus Biologicals, Littleton, CO, USA) counteracted by Fluorescent isothiocyanate (FITC)-conjugated anti-mouse goat secondary antibody (Abcam, Cambridge, MA, USA) to detect expression of total tissue gelatinase A (MMP2), (2) primary non-conjugated human reactive mouse monoclonal anti-matrix metalloproteinase 9 (MMP9) antibody (Novus Biologicals, Littleton, CO, USA) counteracted by phycoerithrene (PE)-conjugated anti-mouse goat secondary antibody (Abcam, Cambridge, MA, USA) to detect expression of total tissue gelatinase B (MMP9) both for invasion and ECM destruction in order to metastasis, (3) primary non-conjugated human reactive mouse monoclonal

anti-vascular endothelial growth factor (VEGF) antibody (Novus Biologicals, Littleton, CO, USA) counteracted by PE-conjugated anti-mouse goat secondary antibody (Abcam, Cambridge, MA, USA) to detect expression of neo-angiogenesis, (4) primary non-conjugated human reactive mouse monoclonal anti-ionized calcium-binding adapter molecule 1 (Iba1) antibody (Abcam, Cambridge, MA, USA) counteracted by FITC-conjugated anti-mouse goat secondary antibody (Abcam, Cambridge, MA, USA) to detect distributional pattern of brain macrophage/microglia, (5) primary PE-conjugated human reactive CD204 mouse monoclonal antibody (BioLegend, San Diego, CA, USA) for detection of M2 polarized brain macrophage or microglia. Subsequently, all of these are counterstained with DAPI (Himedia, India). In all cases 1:500 primary non conjugated and 1:1000 primary or secondary conjugated antibody dilution were used, incubated under dark humid chamber at 4ºC. 5% Fetal Bovine Serum (GIBCO, Life Technology, Grand Island, NY, USA) in 1X PBS with 0.25% Tween 20 (MERCK, India) solution had been used to block nonspecific bindings as well as to increase membrane permeability for cytosolic antibody binding. All the antibodies were diluted in 1% Fetal Bovine Serum FBS (GIBCO, Life Technology, Grand Island, NY, USA) in 1X PBS solution. After mounting in DPX, the slides were viewed through 'Nikon TS 100-F Eclipse' microscope with epi-fluorescence attachment ((Nikon Corp., Japan) using Epi-FL filter block B-2A green channel (Nikon Corp., Japan) for Alexa Fluor® 488 / FITC, Epi-FL filter block G-2A red channel for PE (Nikon Corp., Japan) and UV filter for DAPI (Nikon Corp., Japan) . Photographs of fluorescence stained cells were captured with CCD camera DS-Fi2-U3 (Nikon Corp., Japan), processed, analyzed and documented with 'NIS Element BR' software, version 4.20 (Nikon Corp., Japan).

Glioma Tissue Cell Suspension and Culture

Freshly ablated post-operative human astrocytoma samples were collected in serum free culture medium maintaining aseptic condition and temperature of around 4ºC. Samples were readily minced treated with 0.25% Trypsin-EDTA solution (Sigma Aldrich, USA) and collagenase (HiMedia, India) with continuous agitation. Serum supplemented culture media added to stop the enzymatic process, passed through 70 µm nylon filter mesh (HiMedia, India) and filtrates were centrifuged at 1800 rpm for 3 minutes, pellets washed and dissolved in media and plated for culture in 1X Dulbecco's Modified Eagle Medium (DMEM) supplemented with 15% FBS (MP Biomedicals, Santa Ana, CA, USA), 2% antibiotic-antimycotic solution (HiMedia, India) with use of B-27 cell supplement (GIBCO Life Technologies, USA) with $1.5x10^6$ seeding density in 60 mm cell culture dish (Greiner, Cellstar, Germany) and maintained under 37ºC-5% CO_2 humidified incubator (New Burnswick, Eppendorf, UK). For sets of experiments, 2-3 days of cultured cells were taken, visualized under bright field microscope and prepared subsequently.

Immunocytochemistry (ICC) of Low and High Grade Astrocytoma Primary Culture

After 48 hrs of culture the cells were washed and fixed in 4% paraformaldehyde and added with 5% FBS in PBS with 0.5% Tween-20 (SRL, India) for blocking and permeabilization. After washing, they are treated individually with: (1) mAb Ki67-FITC conjugated antibody for total cell proliferation (2) MMP2 mAb (1^0)-PE (2^0) (3) MMP9 mAb (1^0)-FITC (2^0) for total gelatinase (4) VEGF (1^0)-PE (2^0) for neo-angiogenic endothelial expression as detailed in earlier methodologies. All the antibodies added with a dilution of

1:500 for primary and 1:700 for secondary and incubated for 1 hr each at ambient temperature in dark, counterstained with DAPI and observed under 'Nikon TS 100-F Eclipse' microscope with epi-fluorescence attachment (Nikon Corp., Japan) and captured with CCD camera DS-Fi2-U3 (Nikon Corp., Japan), processed, analyzed and documented with 'NIS Element BR' software, version 4.20 (Nikon Corp., Japan).

Cellular Invasion by Transwell Matrigel Assay in Boyden Chamber

Isolated cells from post-operative tumor tissue were plated at about 0.1 x 10^6 seeding density in serum free 1X DMEM over upper Boyden transwell chamber overlaid with tissue matrigel (Corning, USA) quarterly diluted with serum free DMEM [Ritch et al, 2019]. The lower chamber filled with 1X DMEM+20% FBS+2% antibiotic solution and the preparations were kept at 37ºC-5% CO_2 humified environment for 48 hours. Then the media from lower parts were taken, centrifuged and fixed with 4% paraformaldehyde for immunophenotyping vide flow cytometry (discussed later). Upper chamber withdrawn, fixed similarly, washed and treated with 100% methanol (SRL, India) and stained with 10% giemsa and observed under bright field microscope and documented as mentioned earlier to estimate and compare the invaded cells among low and high grades of astrocytoma.

Cellular Immunophenotyping with Flow-cytometry (FC)

After 48 hours of culture cells were removed by accutase cell detachment solution (Sigma Aldrich, USA) followed by PBS wash and fixation by 4% paraformaldehyde for 15 minutes, washed, pellets were treated with permealizing blocking buffer (5% FBS in PBS+0.5% Tween 20), kept for 45 minutes, washed thoroughly and incubated with: (1) Ki67-FITC conjugated antibody for total cell proliferation (2) MMP2 (1^0)-PE(2^0) (3) MMP9 (1^0)-FITC(2^0) for total gelatinase (4) VEGF(1^0)-PE(2^0) for angiogenic endothelial expression (specification of mAb and conjugates were same as mentioned earlier). After respective incubation of 1 hour each at ambient temperature in dark, pellets were washed, suspended in PBS and fluorescent reading were taken in BD FACS Verse (BD Biosciences, USA) and analyzed with 'FACS Verse Suit 1.0' (BD Biosciences, USA) with calculation of median fluorescence intensity (MFI) for quantification. Same experimental protocols were followed for invading cells recovered from transwell matrigel assay in Boyden chamber for identical parameters to compare with tumor whole tissue parameters.

Isolation of RNA from Tumor Tissue followed by cDNA Conversion

Total RNA were isolated using 'AllPrep Isolation Kit' (Qiagen, India) abiding by manufacturer's protocol from 15 mg frozen tumor tissue of both high and low grade kept in 'RNA later solution' (Thermo Fischer, USA). Isolated RNA quantified in 'Nanodrop' (IMPLEN, Germany) at at 260/280 optical density ($OD_{260/280}$) where OD value $\geq$ 2 were taken. From this quantified RNA samples 50 ng RNA underwent cDNA conversion using 'cDNA conversion kit' (Biobharti Lifesciences, India) following manufacturer's protocol. cDNA were stored at – 20ºC for future use.

Evaluation of mRNA expression by Semi-quantitative Reverse Transcriptase PCR (RT-PCR)

Number of target gene parameters was evaluated by RT-PCR. Respective primers underwent PCR with previously isolated cDNA. Product size of the primers were calculated from ‘NCBI PCR PRIMER BLAST’ and their optimum annealing temperature were determined by array of gradient PCR runs. As per the cDNA primer sequences, CTCATCGCAGATGCCTGGAA (FP) and TTCAGGTAATAGGCACCCTTGAAGA (RP) for MMP2, ACGCACGACGTCTTCCAGTA (FP) and CCACCTGGTTCAACTCACTCC (RP) for MMP9, TGCAGATTATGCGGATCAAACC (FP) and TGCATTCACATTTGTTGTGCTGTAG (RP) for VEGF, TCCTTTGGTGGGCACCTAAGACCTG (FP) and TGATGGTTGAGGTCGTTCCTTGATG (RP) for Ki67, CCCCTGAGCCCTACCGAAT (FP) and CTCGCTGGAGTGGACTTGTG (RP) for DNMT1, GATGATGCTGGGCAAGAGAT (FP) and CCTTCAAATCAGGGCAACTC (RP) for Iba1, CTCCCCTTTTCCCCTTTCTG (FP) and ATCGAGGTCCCACTGGAGAAAGT (RP) for CD204, TCATGAAGTGTGACGTTGACATCCGT (FP) and CCTAGAAGCATTTGCGGTGCACGATG (RP) for β-actin as housekeeping & CAACGGATTTGGTCGTATTGG (FP) and GCAACAATATCCACTTTACCAGAGTTAA (RP) for GAPDH as housekeeping had been used (GAPDH used for qRT-PCR only; for all semi-quantitative PCR, β-actin used as internal control). PCR amplification was done using ‘PCR Green Master Mix’ (Promega, USA) in ‘Surecycler 8800’ PCR machine (Agilent Technologies, USA). β-actin was taken as internal control. The amplified products were run in 10% PAGE, stained in ethidium bromide (EtBr) solution (HiMedia), and photographed in gel imager (Life technologies, USA). Further the different band intensities were quantified using ‘Fiji_ImageJ2’ software (NIH, USA), graphically plotted and interpolated.

Quantification of mRNA Expression Level by Quantitative Real Time PCR (qRT-PCR)

Number of target gene parameters were evaluated by RT-PCR. Respective primers underwent PCR with already isolated cDNA. Product size of the primers were calculated from ‘NCBI PCR PRIMER BLAST’ and their optimum annealing temperature were determined by array of gradient PCR runs as mentioned earlier. ‘SYBR Green I master mix’ (Agilent Technologies, USA) was used as primary source of fluorescent along with ‘ROX’ (Agilent Technologies, USA) as null reference dye diluted in DEPC water (1:100) in ‘AriaMX Real Time PCR cycler’ (Agilent Technologies, USA) with requisite forward and reverse primers, DEPC water and cDNA. GAPDH used as internal housekeeping control. The amplification and melt curve were obtained along with Cq values by analyzing with ‘AriaMX Software v1.0’ (Agilent Technologies, USA). This Cq values had been plotted graphically. The lesser the Cq value, greater will be the expression level.

Statistical Analysis

Both parametric and nonparametric interpolation has been done comparing mean or median values with standard deviation (SD) using the ‘GraphPad InStat’ (GraphPad Software, San Digeo, USA) taking significant one-tail or two-tail p value within 0.05.

Results

Proliferation ability goesinverse from low to high grades and variation between tissues to cellular sub-sets are distinct

As evident both in immunohistochemistry (IHC) and immunofluorescence (IF) studies, the proliferative nature in terms of Ki67 expression found higher in low-grades (LG) to high-grades (HG) (Fig: 1A and 1D respectively) which also seems to be coherent in immunofluorescence based immunocytochemistry (IF-ICC) with the same proliferation marker (Fig: 1B). However as far as the H/E histopathology and MRI data is concerned, hyper-cellularity and nuclear atrophy are highly visible in high-grade glioma and further supported by increased NAA and lactate peak in MR spectroscopy along with T2 enhanced midline shift in MRI (Fig: 1A). Hyper-atrophy nature of nucleus is also visible in IF-ICC in high-grades when stained with DAPI than low-grades (Fig: 1D). The low grade tumor Ki67 mean intensity analyzed by H-DAB IHC was 180.82±11.02 while in case of high grade the value was 40.32±4.87 concerning significant attribution ($p=0.0001$) and has been plotted graphically (Fig: 1C).This unique inverse relation of proliferation among low and high grades has also been supported both by semi-quantitative and qualitative RNA expression data when Ki67 used again as target marker in RT-PCR and qRT-PCR respectively (Fig: 1E and 1F respectively). In RT-PCR, average mRNA expression in low grade tumors found nearly many fold higher with significant p value (0.01) justifying the IHC result. Again the quantitative qRT-PCR showed low expression of Ki67 in terms of higher Cq value in high grade tumors (28.86±0.35) than in low grades (26.52±1.01) showing low Cq value with p value 0.03. As the expression and Cq value is inversely proportional, thus both RT-PCR and qRT-PCR showed increased mRNA expression of Ki67 low grade astroglial tumors than high grades. However an unmatched scenario has been found when flowcytometry (FC) data obtained from the isolated cultured cells of high and low grades of astrocytic tumors. The median fluorescent intensity (MFI) procured from the cells of total whole tissue gave higher FC-MFI value in low grades (52±47.01) than the invaded cells through the matrigel where the MFI value showed 23.66±11.89 depicting low nature of proliferation in invaded sub-types of LG. On the other hand, the MFI value of invaded sub-type of HG sharply rose to 474.33±285.51 compared to its total tissue counterpart (average MFI value is 232.33±111.13). This change of proliferative nature among low and high grade tumors related to their whole tissue and invaded sub-types yields significant ($p=0.04$) level of changes depicting differential nature of proliferation skill of whole tissue glioma cells and their invading subtypes (Fig: 1G).

Gelatinase as microinvasive factor maintains strategic increase from low to high grades but varied in cellular sub-sets

MMP2 and MMP9, the two predominant gelatinases, playing important role in microinvasion or metastasis and degrading ECM causing much lethality has been evaluated. Both immunofluorescence based histochemistry (IF-IHC) and cytochemistry (IF-ICC) show increased level of expression of both the MMPs along the increasing grades (Fig: 2A and 2B respectively) which gets further support from Boyden chamber assay giving higher counts of invaded cells of 49.66±6.34 in higher grades (HG) than lower grades (LG) depicting the average count value of 15.33±2.62 ($p=0.002$). The semi-quantitative (RT-PCR) RNA expression of both MMP2 and MMP9 also showed very significant elevation of gelatinase expression in high grades than low grades (Fig: 2C). The mRNA expression in terms of cDNA band intensity values were 4246.48±65.68 and 3794.05±121.96 in 'ImageJ' analysis for MMP2 and MMP9 for HG respectively with respective significant p values of 0.0009 and 0.0001. Whereas in LG tumors MMP2

and MMP9 expression depicted as 1607.83±414.52 and 1550.83±146.46 respectively. This further got support from the real time PCR giving lower Cq value of 27.89±0.35 and 25.51±0.55 for MMP2 and MMP9 respectively in high grades (higher the expression) in terms of both the gelatinases than the lower grades (30.11±0.67 and 27.73±0.65 respectively for MMP2 and MMP9) with p values 0.01 and 0.02 respectively under the restricted degree of significance of 0.05 (Fig: 2D). Again the grades and cohorts of astrocytic tumors when compared in flow cytometric study taking their MFI, a slight change had been witnessed among the LG tumors within their total and invaded subtypes where expression slightly lowered in LG invaded subtypes (MFI value 207±150.23) than whole tissue (MFI value 363.66±148.60) and in HG groups, expression slightly increased in invaded types ranging it to 154.66±102.29 compared to the HG whole tissue type where MFI value is 120.66±92.90 (Fig: 2E). These results showed the MMP2 and MMP9 expression increases in higher grade glioma tissue environment with mild inverse trends found in invaded cellular subtypes.

VEGF as neo-angiogenic factoris not concurrent with glioma grades

Neo-angiogenesis is essential to sustain tumor and one of the predominant neoangiogenic marker in glioma is VEGF. The expression of VEGF in whole tissue IF-IHC and cellular IF-ICC noted higher expression of the marker in low-grade glioma than their high-grade counterparts (Fig: 3A and 3B). Significant RNA level expression has also been witnessed as the RT-PCR followed by cDNA band expression. In low grades the expression of VEGF mRNA was 1.5 times higher compared to the high grades that was coherent with proliferation in low grades than high grades which has been plotted marking the increased expression in low grades with significant result (p=0.02) (Fig: 3C). Moreover qualitative RNA expression also followed the same trend (Fig: 3D) where Cq value in LG seemed marginally lower of 28.08±0.60 compared to HG tumors (29.35±0.38), indicating higher mRNA expression for VEGF in LG with similar significant difference level (p=0.02) found previously in RT-PCR. All of these analytical cues hinted toward some correlations among level of proliferation and rate of neo-angiogenesis. This notion had also been supported by flow cytometry very clearly where high level of cellular expression of VEGF in terms of MFI had been seen in whole tissue of low grades (709±454.12) and high grades (240±120.54). But there were no significant differences of VEGF expression among the invading subtypes of glioma cells isolated from LG (308.66±222.58) and HG (337±330.37) neoplastic tissue samples (Fig: 3E).

Accumulation of microglia/macrophage and alteration of phenotype with glioma grades

Uncontrolled cellular changes in the tumor microenvironment are also equipped with association of immune cells. Aggregation of highly debated association of brain macrophage or microglia had been addressed at tissue, cell and genomic level. As the tumor grade increased, macrophage number steadily increased in terms of Iba1 expression at tissue level as depicted vide IF-IHC (Fig: 4A). The cDNA band expression of Iba1 value of 8938.85±245.09 was bit higher in high grades compared to lower one (8170.53±319.21) with p value at 0.02 (Fig: 4B) showing a marginal overall increase of glioma associated mocroglia/macrophages in higher grades. In contrast, for M2 microglia/macrophages denoted by CD204, the expression was found drastically higher in HG tumors (7782.93±1026.14)

compared to lower grades (2003.91±820.36) showing about 4 fold increase of M2 phenotype maker (p=0.001). This overall increase of glioma associated microglia/macrophage and high association of pro-tumorogenic M2 phenotype with increasing grades of astrocytoma is shown in Fig: 4B. The quantitative Iba1 mRNA expressional analysis in term of Cq was also showing the similar result (24.5±0.45 in HG and 26.31±0.33 in LG), though the increase of M2 phenotype show marginal differences with CD204 Cq having a lower value of 23.42±0.38 in high grade compared to the low grade Cq value 24.58±0.40 (p=0.04) (Fig:4C). This had given a clear indication of higher presence of microglia/macrophages and their phenotypic with higher glioma grades.

Increased methylation level depicted increased epigenetic alterations in higher grades

Epigenetic associations are considered to be one of the futile player in the up-bringing of the tumor. In our present context, overall level of methylation had been addressed using DNMT1 as marker. Both the H-DAB and IF-IHC showed higher level of DNMT1 expression in high grades (HG) of astrocytoma than low grades (LG); moreover the intensity found from H-DAB IHC had further been plotted graphically (p=0.02) where the DNMT1 mean intensity was 50.35±2.45 in low grade which was much low compared to 108.48±23.83 in high grades (Fig: 5A). The cDNA expression of extracted RNA also gave higher band intensity in high grades. Experimental outcome suggested high level of methylation in HG (21281.15±4201.39) compared to LG (5496.42±186.61) ($p < 0.05$) in terms of the band intensity of DNMT1 (Fig: 5B). Furthermore, low Cq value of 23.78±0.43 yielded from high grades of tumor in comparison to Cq value of 25.33±0.59 in LG ($p < 0.05$) also qualitatively suggested higher expression of DNMT1 in higher grades than in lower grades (Fig: 5C).

Discussion

Tumor is presently considered not only a mass of cell but a heterogeneous tissue-organ-system comprising various other intermingling cells [Egeblad et. al., 2010]. This characteristic is appropriate for the deadly glioma with minimal median survival and such heterogeneity exists in its tissue architecture and assemblage through the grades holistically [Louis et al., 2016; Friedmann-Morvinski, 2014]. With the patient samples of glioma grouped as low-grade (LG) and high-grade (HG) we observed the mentioned principal characteristics of glioma tissue into ‘grow’ and ‘go’ vectors with the presence of glioma associated macrophages/microglia (GAM) on a general epigenetic background marker to understand how such features go concurrently in transforming lower to higher grades of glioma.

Recent evidences suggested that GAM is highly interactive and influentially alter the micro-environmental status and progressive behavior in glioma by influencing angiogenic and invasive properties in glioma. Such association of microglia and infiltrated macrophage with M2 phenotypes expressing $CD163^+$, $CD204^+$ or $CD206^+$ has been found related with aggressive behavior and poor prognosis [Miyasato et al., 2017; Sørensen et al, 2018; Matias et al., 2018]. GAM was found abundant with increasing grades and correlated with hypoxia inducible factor (HIF) and matrix metalloproteases (MMPs) family members like MMP 2, 9 and 14 controlling its aggression and invasiveness [Rao, 2003; Lettau et al, 2010;Hagemann et

al, 2012; Ghosh et al., 2017]. In relation to HIF during glioma growth, its sustenance is induced by VEGF by promoting angiogenesis, vascular permeability, contributing in formation of immunosuppressive microenvironment by inhibiting dencritic cell (DC) maturation and expressing death receptor PD-L1 [Miki et al, 2012; Xue et al, 2017]. So vascular permeability in turn increases the access of GAM into tumor microenvironment and secreting IL-6, IL-10, TGF-β, EGF, VEGF, MMP 2, 4 and 9, where CX3CR1 or CCR2 etc influencing their movement receiving glioma secreting CX3CL1, CCL2 etc, hence producing a vicious spiral of glioma-GAM carnage [Ghosh and Chaudhuri, 2010; Zhang et al, 2012; Ferrer et al, 2018; Matias et al., 2018]. Therefore, dangerously growing glioma causing massive CNS tissue architectural destruction in higher grades possesses multifaceted but interrelated mechanisms. Gradually the participating factors in this entangled process are being exposed with their functions in transformation from lower to higher grades of glioma. In this scenario, the proliferation-invasion arms of glioma growth have shown some Yin-Yang feature with tentative variations in their invading subsets.

The tumor growth when measured with proliferative features among the samples of low to high grade gliomas using one of the most widely used proliferation marker Ki67, high proliferative rates observed among both groups, but remarkably higher proliferative potency was observed in lower grades than the higher grade samples. Such observation was cross-checked for whole glioma tissue samples using multiple technical approaches to document the fact at cellular protein and mRNA level expression finding similar trend with some deviation in magnitude (Fig. 1). But selective cells in 2-3 days culture from lower grade tissue samples showed less Ki67 protein expression in flow cytometry than higher grades indicating consistency with existing observations where Ki67 manifestation rises with glioma grades [Skjulsvik et al, 2014]. In contrast, when invading cellular sub-types of both grades are compared with their parent populations in culture, invading glioma cells of lower grades were found less proliferative to its whole tissue culture survived cells; whereas, the invading cells from high-grade glioma are highly proliferative and even much higher than the high proliferative whole tissue culture survived cells of high-grade gliomas (Fig. 1G and Fig.6). This disparity among the proliferative surge among the whole tissue, selective survived cells in culture and their invading sub-sets are showing the heterogeneous properties of behavioral variants within the same glioma tissue indicating a clonal heterogeneity on behavioral pattern [Friedmann-Morvinski, 2014].

Growth by proliferation is not the only vector that make glioma so dangerous, rather the aggressive invading property of it made the issue nearly invincible with recurrence particularly in higher grades. In a tumor niche, with proliferation ECM degrading enzymes are pressed into service among which gelatinases like MMP2 and MMP9 are most predominant in glioma, which usually gets inactivated by TIMPs and gets activated once the condition arises controlling their cysteine switches and also having cytokine-chemokine dependent axis of activation [Toth et. al., 2003; Coniglio and Segall, 2013; Zhang et al, 2012; Ferrer et al, 2018]. Folds increase of both MMP2 and MMP9 expression are observed from lower to higher grades in glioma tissue at protein and mRNA level, indicating highly aggressive and invading state at tissue level as depicted in Fig. 2. But the scenario flipped when selective cells surviving in culture showed higher MMP expression for lower grades, which is remarkably an exact reverse behavior against proliferative potency as seen earlier (Fig. 6). Though such reverse trend is observed for invading subsets

of glioma cells between lower and higher cohorts of samples, but the difference in invading potency is mild, particularly in comparison to proliferation. Therefore, the behavior of overall glioma tissue mass and selective behavioral subsets distinctly varies in their invading capacity, along with, showing a dichotomous relation for the ‘grow’ and ‘go’ vectors in growing glioma. To mitigate the discrepancy with whole tissue and its culture sustained glioma cells or invading cell subsets, the role of other contributing cellular components including the candid role of GAM are expected crucial. They are capable to producing excessive MMPs in high-grade gliomas [Arcuri et al, 2017]. Glioblastoma cells expressing CX3CL1 induces GAM recruitment through CX3CR1 receptors with resultant increase in MMP 2, 9 and 14, thereby promoting an invading microenvironment for glioma surroundings [da Fonseca and Badie, 2013; Ferrer et al, 2018]. Differential expression of MMP9 along with the molecular subtypes of breast cancer had been reported [Pellikainen et. al., 2004; Yousef et. al., 2014] and such alternating subtypes are presumably factual for astrocytic tumor in a more complex way as indicated through the observations.

Cellular proliferation is an energy driven process requiring high level of gaseous and nutritional supply through neoangiogenesis that is critically dependent upon oxygen tension sensed by various mechanisms, including NADPH oxidases, endothelial nitric-oxide synthase (eNOS), heme-oxygenases and oxygen sensors that interface with the hypoxia-inducible transcription factor HIFα (HIF-1–3) family hetero-dimerizing with aryl hydrocarbon receptor nuclear translocator (HIFβ/ARNT) subunit [Semenza, 2003; Ward, 2008]. In growing cancers, endothelial cells are vigorously active releasing several factors such as EGF, FGF, IL-8, prostaglandin E1 and E2, TNF-α, and VEGF, that can activate endothelial cell growth and motility where VEGF and bFGF are particularly important to tumor angiogenesis.In CNS astrocytes release various molecular mediators, such prostaglandins (PGE), nitric oxide (NO), and arachidonic acid (AA) influencing CNS blood vessel diameter and neo-angiogenesis where constantly secreting VEGF and allies from glioma cells promote its own growth by recruiting GAM[Gordon et. al., 2007; Rajabi & Mousa, 2017; Arcuri et al, 2017]. VEGF expression in the whole tumor tissue shows an overall decline from lower to higher grades as observed in immunohistochemistry IHC or in RNA level expression of the factor, where surviving cells from whole sample culture also follows the similar trend (Fig. 3). This behavior of whole sample VEGF is supporting the trend of Ki67 observed earlier and correlating angiogenesis with proliferation, but disparity in angiogenic and proliferation marker for glioma tissue cells survived in culture may need further explanation involving other cellular components released factors, namely, astrocytes, epithelial cells or GAMs [Argaw et al, 2012; Osterberg et al, 2016; Rajabi & Mousa, 2017; Arcuri et al, 2017]. Interestingly, the invading cell in culture shows consistency in their VEGF expression, rather moderately increased VEGF is observed in higher grades associating its expression with high proliferative potency of those cells (Fig. 3 and 6), indicating their essential presence in immediately invaded microenvironment where rapid proliferation require neo-angiogenic support to colonize and sustain. VEGF induces PI3K/Akt and Ras/MAPK mediated mitogenic pathway for growth of glioma cells, as well as, activation of MMPs for ECM remodeling as already established, thereby, mitigating both high proliferative urges of cellsof high-grade glioma when invades in newer regions and associated MMP secretion in high amount from that tissue microenvironment in that phase [Wong et al, 2009; Xu et al, 2013].

The entire glioma milieu develops on a dynamic genetic contour and controlled by various epigenetic gears that are participating from various cellular subsets of the tumor microenvironment. In recent times, such epigenetic controls are significantly contributing to understand tumor biology for their ability to control gene expression levels as holistic or specific means by chromatin remodeling or RNA interference and strategically developing as markers to identify DNA methylation, histone modifications, chromatin remodeling, and microRNA for cancer development and progression [Nebbioso et. al., 2018]. DNA methylation was one of the earliest epigenetic markers in different cancers including glioma which are linked to control many genes like CDKN2A, TP53, TP73, MGMT, PTEN, Rb, TIMP3, MMP9 etc as identified so far and may increase ROS which in turn activate DNMT for further methylation [Rajendran et. al., 2011; Caffo et. al., 2014; Rasime 2015; Ghosh et al, 2017]. Present study showed high increase of methylation pattern in glioma tissue of higher grades with clustered enhanced DNMT1 expression at protein levels which has also been reflected in mRNA production level, but here the difference is less (Fig. 5). Such epigenetic perturbation in higher grades have several mechanisms including the involvement of microRNAs like miR21, miR451, miR663 etc secreting in glioma microenvironment and/or modulate both glioma cells and GAM involving AMPK, mTOR, or through TGFβ mediated MMP2, E-cadherin dependent microinvasion processes [Baraniskin et al, 2012; Li et al, 2016; Zhao et al, 2017]. Also the secreted extracellular vesicles (EVs) in glioma microenvironment derived from different cellular participant crosstalk and influence each other, and preliminary knowledge in such area indicates their role in controlling glioma aggressiveness and GAM polarization [Drago et al, 2017; Matias et al., 2018]. Therefore, such epigenetic background and active influences from glioma microenvironment derived factors, as already described, not only facilitate the recruitment of microglia or macrophages in increasing numbers but also induce their polarization process. Such increased GAM with $Iba1^+$ immune-phenotype has been observed with predominant presence of $CD204^+$ cells of M2 polarization for high-grade glioma samples (Fig. 4) in accordance with other studies [Komohara et al, 2008; Ghosh et al, 2016; Miyasato et al, 2017]. This high presence of microglia/macrophages had long being designated with the increase or aggression of glioma where M2 polarized subsets are now considered to play the pivotal role in transforming glioma to higher grade features [Ghosh and Chaudhuri, 2010; Wei et al, 2013; Matias et al, 2018]. Evidences showed that hyper-activation of a subtype of M2 polarized GAM, designated as M2c, by tumor cell secreted IL-10, TGF-β, and glucocorticoids subsequently act through STAT3, FIZZ1 or PPAR-γ mediated signaling pathways, which induces ECM digestion and tissue remodeling by the expression of versican, antitrypsin, gelatinase and pentraxin 3 and facilitate neo-angiogenesis, tumor growth, migration and invasion to an immunosuppressive microenvironment [Hambardzumyan et. al., 2016; Orihuela et. al., 2016].

So the interrelationship of mentioned features and predicted dichotomy does not go straight from low to high grade transition of glioma and cellular variants of tumor tissue come into play to the behavioral pursuit of glioma aggression. Overall, in an increasingly perturbed epigenetic landscape infested with myeloid lineage derived innate immune cells that are mostly polarized towards M2 phenotype in lower and higher grades of glioma tissue microenvironment, the hallmark features of its aggression shows tissue and cellular subtype specific variability or heterogeneity. When lower grade glioma is found to be

inclined towards growth as marked by the increased expression of proliferation markers, higher grade glioma, in contrast, has been found to be more aggressive and invasive at the whole tissue levels (Fig. 6). But such trend get inversed when selective culture survived glioma cells are compared from both cohorts, where cells from higher-grades found more proliferative and its invading subtypes possess prolific capacity to grow, but the metastatic properties show the reverse trend for both the derived subtypes as schematically depicted in Fig. 6. Proliferative trends are highly supported by angiogenesis as shown by VEGF expression, however higher contributions of other members in this process can be predicted as discussed previously. So the cellular behavior distinctly varies within the glioma microenvironment where a tissue level and cellular level dichotomy between ‘grow’ and ‘go’ exists, in which, a tissue level decision may not coincide with the cellular components of the organotypic tumor whole. Such glioma microenvironmental heterogeneity at the level of genetic expression in a niche specific manner has been under strict scrutiny in the present years to develop better therapeutic strategy [Friedmann-Morvinski, 2014; Perrin, 2019], but heterogeneity among behavioral subsets of cells from lower to higher grade glioma with dichotomous relation indicating a decision making juncture may also be exploited for future prognostic measures. Present study in tumor samples also indicates the mathematical modeling predicting the switching of glioma to the invasive phenotype and migrating toward adjacent brain, and switching back to proliferating cells may hold substantive factual evidences in real time [Hatzikirou et al, 2012; Saut et al, 2014], however, further detailing on larger samples are required to establish any such dichotomy and switching. In this whole endeavor by glioma, its neoplastic cellular components, associated microglia/macrophage, astrocytes, epithelial cells with their products and varieties of ECM mediators play a great role where someone is hijacking and influencing others action and the triumph of glioma has made its way [Gieryng et al, 2017; Arcuri et al., 2017; Matias et al., 2018]. Understanding the mode of action of cellular components and their operational dichotomy or coupling in this multifaceted dynamic glioma environment in lower to higher phase transition may provide additional insight for better therapeutic interventions to combat this deadly malaise.

Declarations

Funding: This work was supported by the Council of Scientific and Industrial Research (CSIR), Government of India for financial aid vide Sanction No. 37(1587)/13/EMR-II dated 01.04.2013 to Anirban Ghosh as Principal Investigator (PI) for the work.

Declaration of Conflict of interest / competing interest: The authors declare that they have no known competing financial interests or personal relationships that could have appeared to influence the work reported in this paper.

Ethics approval and consent to participate: Working with the post-operative human tumor samples, authors abide by patients’ consent proposal and Human Ethical Clearance (Memo No: *Inst/IEC/553 dated 15.01.2014*) from Institutional Ethical Committee (IEC) at Institute of Post Graduate Medical Education and Research (IPGME&R), Kolkata, West Bengal, India legally validating World Medical Association (WMA), Declaration of Helsinki.

Consent for publication: NA

Availability of data and material: Data provided in the manuscript and if required further, will be provided by the first and corresponding authors.

Code availability: NA

Authors' Contribution: KG primarily performed the experiments as designed by AG, acquired and analyzed data and drafted the initial manuscript; SG provided post-surgical samples and MRI data; UC have done histopathological analysis; PB provided few experimental facilities to KG and mentored him; AG planned the whole work with acquisition of fund, mentored KG and supervised the whole work and experiments, analyzed data and finalized the manuscript draft.

Acknowledgements: Acknowledging M.Ch students at Neurosurgery unit, BIN, IPGME&R for post-operative tumor samples, Dr. Ritesh Tiwari of BD-CoE Flow Cytometry unit at CRNN, University of Calcutta for immuno-flowcytometry experiments and analysis. Sincere gratitude to Prof. Asis Kumar Chattopadhyay and Ms. Soumita Modak, Department of Statistics, University of Calcutta for helping in statistical interpretation. Authors also thank Mr. Sanku Mondal and Mr. Abir Roy for their suggestions in preparing the figures for the manuscript.

References

1. Arcuri C, Fioretti B. Bianchi R et al (2017) Microglia-glioma cross-talk: a two way approach to new strategies against glioma. Front Biosci-Landmrk 22: 268-309.
2. Argaw AT, Asp L, Zhang J et al (2012) Astrocyte-derived VEGF-A drives blood-brain barrier disruption in CNS inflammatory disease. J Clin Invest 122: 2454-2468. (doi:10.1172/JCI60842)
3. Baraniskin A, Kuhnhenn J, Schlegel U, Maghnouj A, Zöllner H, Schmiegel W, Hahn S, Schroers R (2012) Identification of microRNAs in the cerebrospinal fluid as biomarker for the diagnosis of glioma. Neuro Oncol 14: 29-33. (DOI: 10.1093/neuonc/nor169)
4. Caffo M, Caruso G, La Fata G, Barresi V, Visalli M, Venza M, Venza I (2014) Heavy metals and epigenetic alterations in brain tumors. Current Genomics 15: 457-463.
5. da Fonseca ACC, Badie B (2013) Microglia and Macrophages in Malignant Gliomas: Recent Discoveries and Implications for Promising Therapies. Clin Dev Immunol (J Immunol Res) Article ID 264124, http://dx.doi.org/10.1155/2013/264124.
6. Drago F, Lombardi M, Prada I, et al (2017) ATP modifies the proteome of extracellular vesicles released by microglia and influences their action on astrocytes. Front Pharmacol 8: 910. (doi: 10.3389/fphar.2017.00910)
7. Egeblad M, Nakasone ES, Werb Z (2010) Tumors as organs: complex tissues that interface with the entire organism. Dev Cell 18: 884-901.

8. Ferrer VP, Moura Neto V, Mentlein R (2018) Glioma infiltration and extracellular matrix: key players and modulators. Glia 66: 1542–1565. (doi: 10.1002/glia.23309)
9. Friedmann-Morvinski D (2014) Glioblastoma heterogeneity and cancer cell plasticity. Crit Rev Oncog 19(5): 327-36. (doi: 10.1615/critrevoncog.2014011777)
10. Gajewski TF, Schreiber H, Fu Y-X (2013). Innate and adaptive immune cells in the tumor microenvironment. Nat Immunol 14(10): 1014–22. (doi:10.1038/ ni.2703)
11. Ghosh A, Chaudhuri S (2010) Microglial action in glioma: a boon turns bane. Immunol Lett 131: 3-9. (DOI: 10.1016/j.imlet.2010.03.003)
12. Ghosh K, Bhattacharjee P, Ghosh S, Ghosh A (2017) Glia to glioma: A wrathful journey. Adv Mod Oncol Res 3: 96-113. (DOI:10.18282/amor.v3.i3.186)
13. Ghosh K, Ghosh S, Chatterjee U, Chaudhuri S, Ghosh A (2016) Microglial Contribution to Glioma Progression: an Immunohistochemical Study in Eastern India. APJCP 17(6): 2767-73.
14. Gieryng A, Pszczolkowska D, Walentynowicz KA, Rajan WD, Kaminska B (2017) Immune microenvironment of gliomas. Lab Invest 97: 498-518.
15. Giese A, Bjerkvig M, Behrens M, Westphal M (2003) Cost of Migration: invasion of malignant gliomas and implication for treatment. J Clin Oncol 21: 1624-1636.
16. Gordon GR, Mulligan SJ, MacVicar BA (2007) Astrocyte control of the cerebrovasculature. Glia 55: 1214-21.
17. Hagemann C, Anacker J, Ernestus RI, Vince GH (2012) A Complete Compilation of Matrix Metalloproteinase Expression in Human Malignant Gliomas. World J Clin Oncol 3(5): 67-79.
18. Hambardzumyan D, Gutmann DH, Kettenmann H (2016) The role of microglia and macrophages in glioma maintenance and progression. Nat Neurosci 19(1): 20-27.
19. Hanahan D, Weinberg RA (2011) Hallmarks of cancer: the next generation. Cell 144: 646-74.
20. Hatzikirou H, Basanta D, Simon M, Schaller K, Deutsch A (2012) 'Go or grow': the key to the emergence of invasion in tumour progression? Math Med Biol 29:49–65.
21. Komohara Y, Ohnishi K, Kuratsu J, Takeya M (2008) Possible involvement of the M2 antiinflammatory macrophage phenotype in growth of human gliomas. J Pathol216: 15-24. (doi:10.1002/path.2370)
22. Lettau I, Hattermann K, Held-Feindt J, Brauer R, Sedlacek R, Mentlein R (2010) Matrix Metalloproteinase-19 is Highly Expressed in Astroglial Tumors and Promotes Invasion of Glioma Cells. J Neuropathol Exp Neurol 69: 215-223. (https://doi.org/10.1097/NEN.0b013e3181ce9f67)
23. Li Q, Cheng Q, Chen Z et al (2016) MicroRNA-663 inhibits the proliferation, migration and invasion of glioblastoma cells via targeting TGF-beta1. Oncol Rep 35: 1125–1134. (doi: 10.3892/or.2015.4432)
24. Louis DN (2006) Molecular pathology of malignant gliomas. Annu Rev Pathol Mech Dis 1: 97–117. (doi: 10.1146/annurev.pathol.1.110304.100043)
25. Louis DN, Perry A, Reifenberger G et al (2016) The 2016 World Health Organization classification of tumors of the central nervous system: A summary. Acta Neuropathol 131: 803-20.

26. Matias D, Balça-Silva J, da Graça GC et al (2018). Microglia/Astrocytes–Glioblastoma Crosstalk: Crucial Molecular Mechanisms and Microenvironmental Factors. Front Cell Neurosci 12: 235. (doi:10.3389/fncel.2018.00235)
27. Miki T, Wada M, Kasumimoto T, Moriyama R, Iwasaki Y (2012) Modulation of immunity by antiangiogenic molecules in cancer. Clin Dev Immunol (J Immunol Res) Article ID: 492920. (doi: 10.1155/2012/492920)
28. Miyasato Y, Shiota T, Ohnishi K et al (2017) High density of CD204-positive macrophages predicts worse clinical prognosis in patients with breast cancer. Cancer Sci 108: 1693–1700. (doi: 10.1111/cas.13287)
29. Murat A, Migliavacca E, Hussain SF et al (2009) Modulation of Angiogenic and Inflammatory Response in Glioblastoma by Hypoxia. PLoS ONE 4(6): e5947. (doi:10.1371/journal.pone.0005947)
30. Nallanthighal S, Heiserman JP and Cheon D-J (2019). The Role of the Extracellular Matrix in Cancer Stemness. Front. Cell Dev. Biol. 7:86. (doi: 10.3389/fcell.2019.00086)
31. Nebbioso A, Tambaro FP, Dell'Aversana, C, Altucci L (2018) Cancer epigenetics: Moving forward. PLoS Genet 14(6): e1007362. (https://doi.org/10.1371/journal.pgen.1007362)
32. Orihuela R, McPherson CA, Harry GJ (2016) Microglial M1/M2 polarization and metabolic states. Br J pharmacol 173(4): 649-65.
33. Osterberg N, Ferrara N, Vacher J et al (2016) Decrease of VEGF-A in myeloid cells attenuates glioma progression and prolongs survival in an experimental glioma model. Neuro Oncol 18: 939–949. (doi: 10.1093/neuonc/now005)
34. Ostrom QT, Bauchet L, Davis FG et al (2014) The epidemiology of glioma in adults: a “state of the science” review. NeuroOncol 16(7): 896 –913. (doi:10.1093/neuonc/nou087)
35. Pellikainen JM, Ropponen KM, Kataja VV, Kellokoski JK, Eskelinen MJ, Kosma VM (2004) Expression of matrix metalloproteinase (MMP)-2 and MMP-9 in breast cancer with a special reference to activator protein-2, HER2, and prognosis. Clin Cancer Res 10: 7621-8.
36. Perrin SL, Samuel MS, Koszyca B et al (2019) Glioblastoma heterogeneity and the tumour microenvironment: implications for preclinical research and development of new treatments. Biochem Soc Trans 47: 625-638.
37. Rajabi M, Mousa S (2017) The role of angiogenesis in cancer treatment. Biomedicines 5: 34. (doi:10.3390/biomedicines5020034)
38. Rajendran G, Shanmuganandam K, Bendre A, Mujumdar D, Goel A, Shiras A (2011) Epigenetic regulation of DNA methyltransferases: DNMT1 and DNMT3B in gliomas: J Neuro Oncol 104(2): 483-494.
39. Ramachandran RK, Sørensen MD, Aaberg-Jessen C, Hermansen SK, Kristensen BW (2017) Expression and prognostic impact of matrix metalloproteinase-2 (MMP-2) in astrocytomas. PLoS ONE 12(2): e0172234. (doi:10.1371/journal.pone.0172234)
40. Rao JS (2003) Molecular mechanisms of glioma invasiveness: the role of proteases. Nat Rev Canc 3: 489-501.

41. Rasime K (2015) Epigenetics of Glioblastoma Multiforme. J Clinic Res Bioeth 6 (DOI: 10.4172/2155-9627.1000225).
42. Ritch SJ, Brandhagen BN, Goyeneche AA, Telleria CM (2019). Advanced assessment of migration and invasion of cancer cells in response to mifepristone therapy using double fluorescence cytochemical labelling. BMC Cancer 19:376 (doi: 10.1186/s12885-019-5587-3).
43. Saut O, Lagaert JB, Colin T, Fathallah-Shaykh HM (2014) A multilayer grow-or-go model for GBM: effects of invasive cells and anti-angiogenesis on growth. Bulletin of Mathematical Biology. 76(9): 2306-33.
44. Semenza GL (2003) Targeting HIF-1 for cancer therapy. Nat Rev Cancer 3(10):721-32.
45. Skjulsvik AJ, Mørk JN, Torp MO, Torp SH (2014) Ki-67/MIB-1 immunostaining in a cohort of human gliomas. Int J Clin Exp Pathol 7(12): 8905-8910.
46. Sørensen MD, Dahlrot RH, Boldt HB, Hansen S, Kristensen W (2018) Tumour-associated microglia/macrophages predict poor prognosis in high-grade gliomas and correlate with an aggressive tumour subtype. Neuropathol Appl Neurobiol 44: 185-206. (doi: 10.1111/nan.12428)
47. Stuelten CH, Parent CA and Montell DJ (2018). Cell motility in cancer invasion and metastasis: insights from simple model organisms. Nat Rev Cancer 18: 296-312. (doi:10.1038/nrc.2018.15)
48. Toth M, Chvyrkova I, Bernardo MM, Hernandez-Barrantes S, Fridman R (2003) Pro-MMP-9 activation by the MT1-MMP/MMP-2 axis and MMP-3: role of TIMP-2 and plasma membranes. Biochem Biophys Res Co 308: 386-95.
49. Ward JP (2008) Oxygen sensors in context. BBA-Bioenergetics 1777:1-4.
50. Wei J, Gabrusiewicz K, Heimberger A (2013) The Controversial Role of Microglia in Malignant Gliomas. Clin Dev Immunol (J Immunol Res) Article ID 285246. (http://dx.doi.org/10.1155/2013/285246)
51. Wild-Bode C, Weller M, Wick W (2001) Molecular Determinants of Glioma Cell Migration and Invasion. J Neurosurg 94(6): 978-984.
52. Wong ML, Prawira A, Kaye AH, Hovens CM (2009) Tumour Angiogenesis: its Mechanism and Therapeutic Implications in Malignant Gliomas. J Clin Neurosci 16: 1119-1130.
53. Xu C, Wu X, Zhu J (2013) VEGF Promotes Proliferation of Human Glioblastoma Multiforme Stem-Like Cells through VEGF Receptor 2. Sci World J Article ID 417413. (doi: 10.1155/2013/417413)
54. Xue S, Hu M, Li P et al (2017)Relationship between expression of PD-L1 and tumor angiogenesis, proliferation, and invasion in glioma.Oncotarget 8: 49702-49712.
55. Yousef EM, Tahir MR, St-Pierre Y, Gaboury LA (2014) MMP-9 expression varies according to molecular subtypes of breast cancer. BMC Cancer 14:609. (DOI: 10.1186/1471-2407-14-609)
56. Yuan Y, Xiang W, Yanhui L et al (2013) Ki-67 overexpression in WHO grade II gliomas is associated with poor postoperative seizure control. Seizure 22: 877–881.
57. Zhang J, Sarkar S, Cua R, Zhou Y, Hader W, Yong V W (2012) A dialog between glioma and microglia that promotes tumor invasiveness through the CCL2/CCR2/interleukin-6 axis. Carcinogenesis 33:

312–319. (doi: 10.1093/carcin/bgr289)

58. Zhao K, Wang L, Li T et al (2017) The role of miR-451 in the switching between proliferation and migration in malignant glioma cells: AMPK signaling, mTOR modulation and Rac1 activation required. Int J Oncol 50: 1989–1999.

Figures

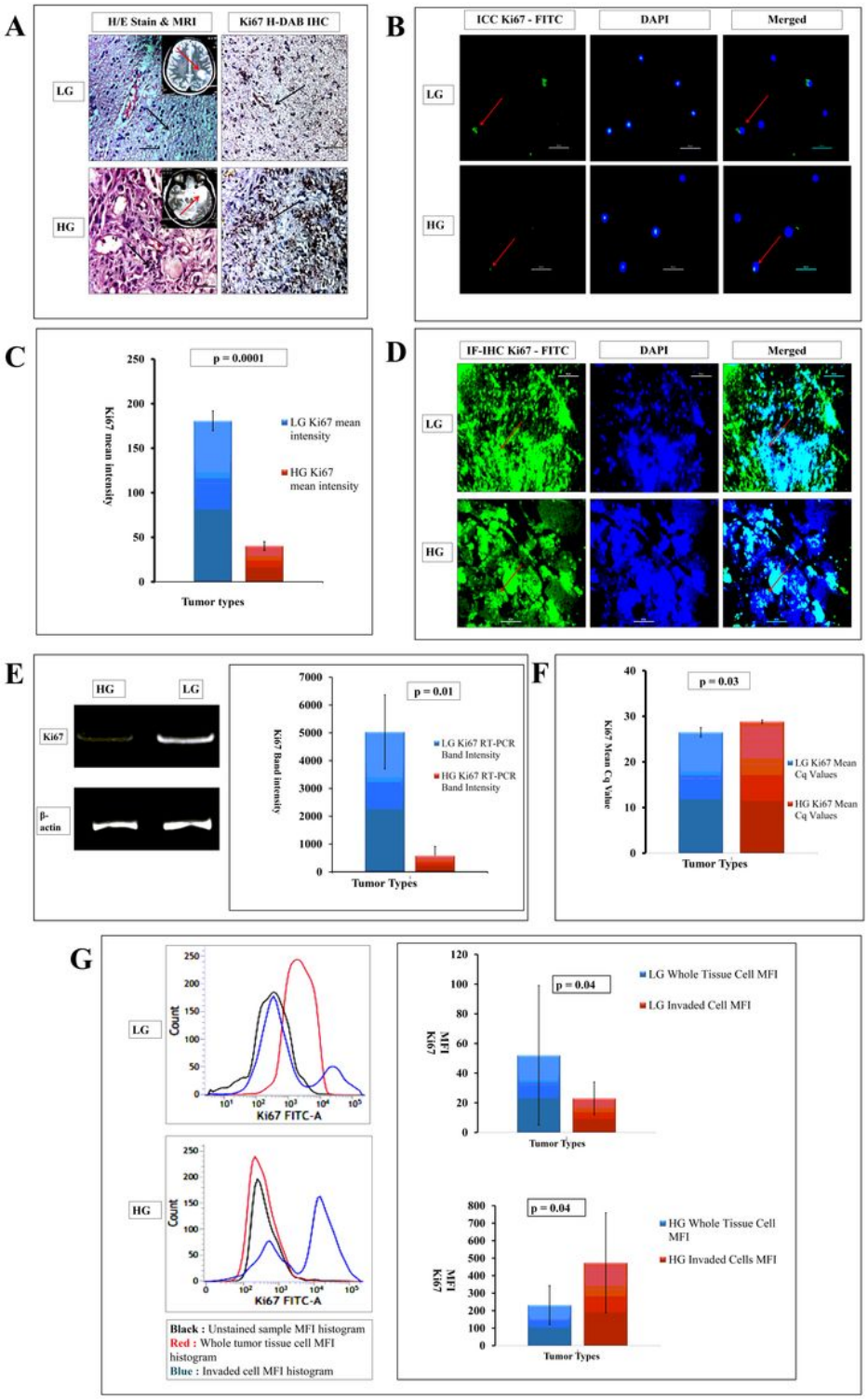

Figure 1

[A] Hematoxylin-Eosine (H/E) stained histopathology (400X) shows increasing hypercellularity and distortion of cellular matrix (black arrow) in low (LG) and high (HG) grade glioma. Respective T2 weighted MRI images [inset] are showing the lesions (red arrow). Hyper-expressive areas with H-DAB Ki67 IHC has been seen in low-grade gliomas more dominantly than high-grade gliomas (HG). [B]Immunocytochemistry (ICC) with Ki67-FITC and DAPI also showing hyper expression of the said proliferative marker in LG (red arrow). [C] Graphical plot of Ki67 mean intensity found in H-DAB Ki67 IHC with p value of 0.0001 depicts significant higher expression in LG. [D] Whole tissue IF-IHC with Ki67-FITC and DAPI (400X) also points out higher level of proliferation in LG (red arrows). [E] cDNA band expression (extreme left) of RNA transcript of Ki67 suggests hyper expression (middle) with p value of 0.01 in LG tumors. [F] Lower Cq value found in qRT-PCR in LG tumors denotes hyper expression of Ki67 as proliferation marker. [G]Medianfluorescent intensity (MFI) values (p 0.04) of Ki67 found in LG and HG whole tumors and their invaded cohorts - Ki67 expression in whole tumor tissue of LG is higher, however the invaded cells of HG show high shoots of the expression compared to its whole tissue cell type.

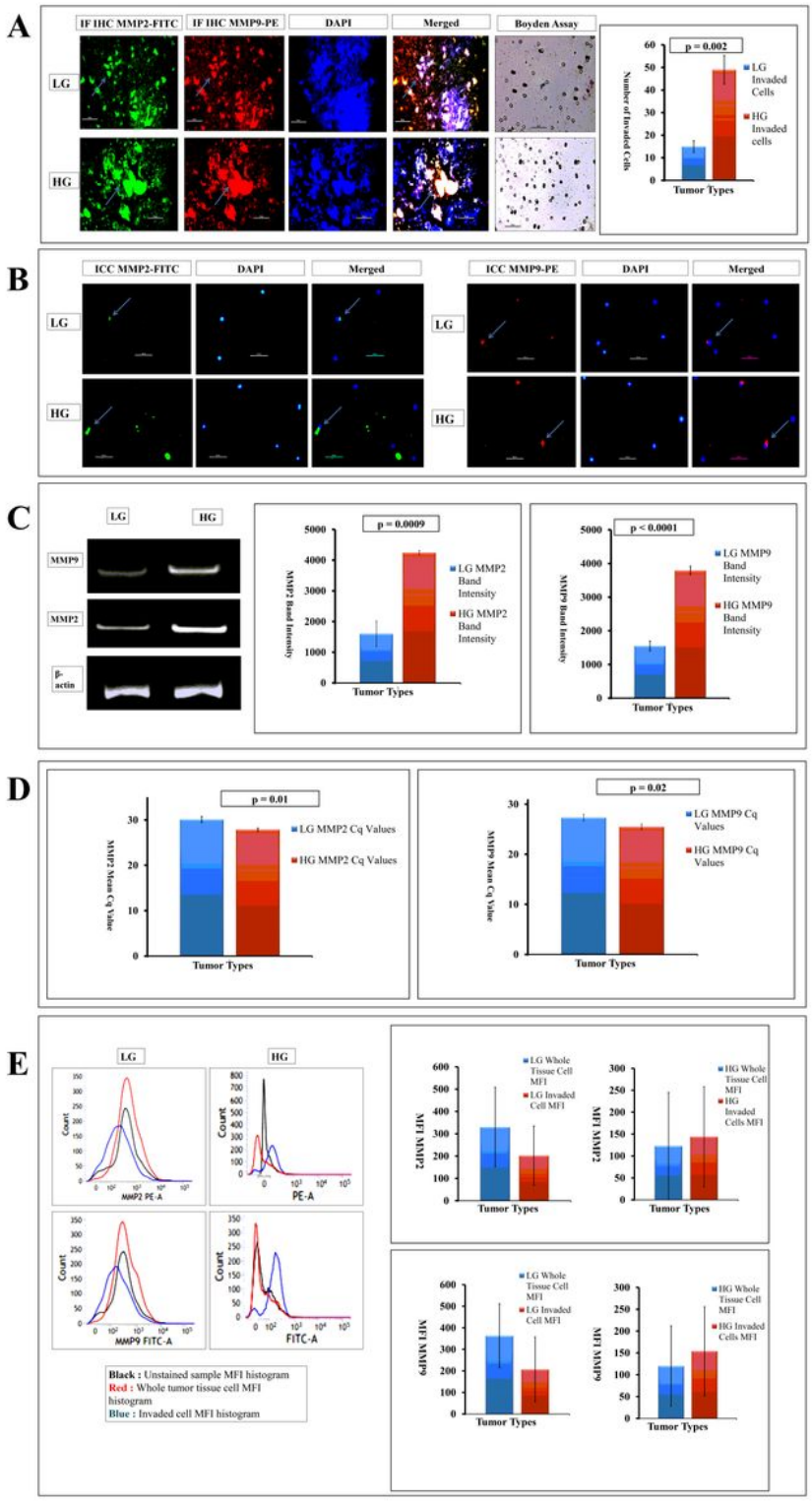

Figure 2

[A] Whole tissue IF-IHC with MMP2-FITC and MMP9-PE contrasted with DAPI (marked with sky blue arrow) suggests increasing expression of both the gelatinases from low (LG) to high (HG) grades (400X). The transwell assay also shows higher number of invaded cells in HG than LG with significant p value of 0.002 (after 24 hours from overlay). [B] Concurrent higher expression found in HG tumors in ICC with MMP2-FITC and MMP9-PE along with DAPI (marked with sky blue arrow) (400X). [C] Quantitative RNA

expression of both the MMP2 and MMP9 shows higher expression in HG than in LG tumors taking β-actin as housekeeping gene with very significant expression profiling (p value is 0.0009 and less than 0.0001 respectively). [D] Both MMP2 and MMP9 qPCR data shows low Cq values in high grades depicting hyper expression than low grades (p value 0.01 and 0.02 respectively). [E] In MFI expression using MMP2-PE and MMP9-FITC, the changes are visible among total and invaded cells. In MMP2, the MFI found in the LG whole tissue cell is higher than invaded sub-type; while in HG, MMP2 expression is higher in invaded sub-type than the whole tissue cell. On the other hand, MMP9 expression also shows similar expression as in LG, the invaded type shows lower expression than whole tissue, while slight increase in MMP9 expression has been witnessed in invaded cells of HG than its whole cell counterpart ($p \geq 0.05$).

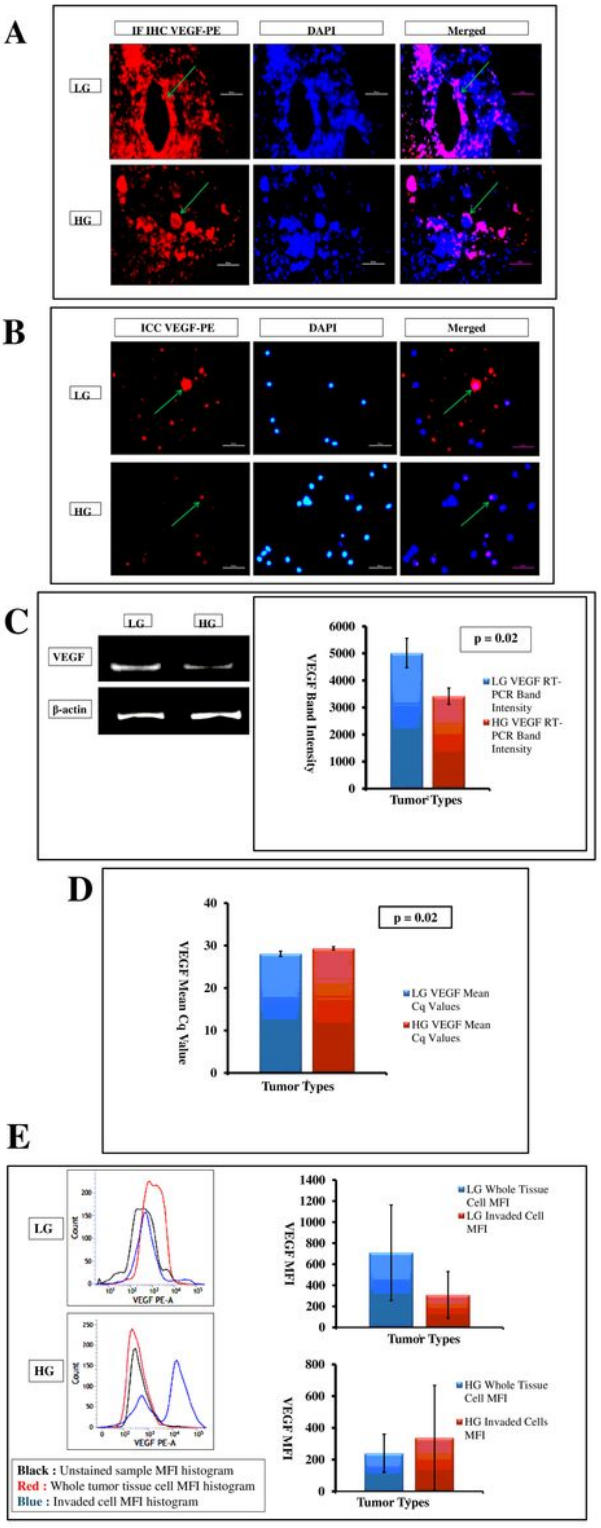

Figure 3

[A] Whole tissue IF-IHC with VEGF-PE and DAPI (400X, marked with green arrows) shows increased level of neoangiogenic expression in low grades (LG) rather high grades (HG). [B] ICC with isolated cells from tumor tissue also show increased level of VEGF expression (400X, marked with green arrows) in LG tumors than their HG counterparts. [C] cDNA gel band expression taking VEGF as target and β-actin as housekeeping, depicts higher level of capillary sprouting in LG tumors with p value of 0.02. [D] RNA

expression by qRT-PCR suggests high Cq value in high grade tumors indicating their lower level of neoangiogenic ability than LG tumors (p=0.02). [E] MFI of VEGF in flowcytometry is concurrent with proliferation. In LG tumor, the expression is higher in whole tissue cell than the invaded counterparts; while in HG tumors, the level of angiogenic expression is higher in invaded cells than whole tissue cells ($p \geq 0.05$).

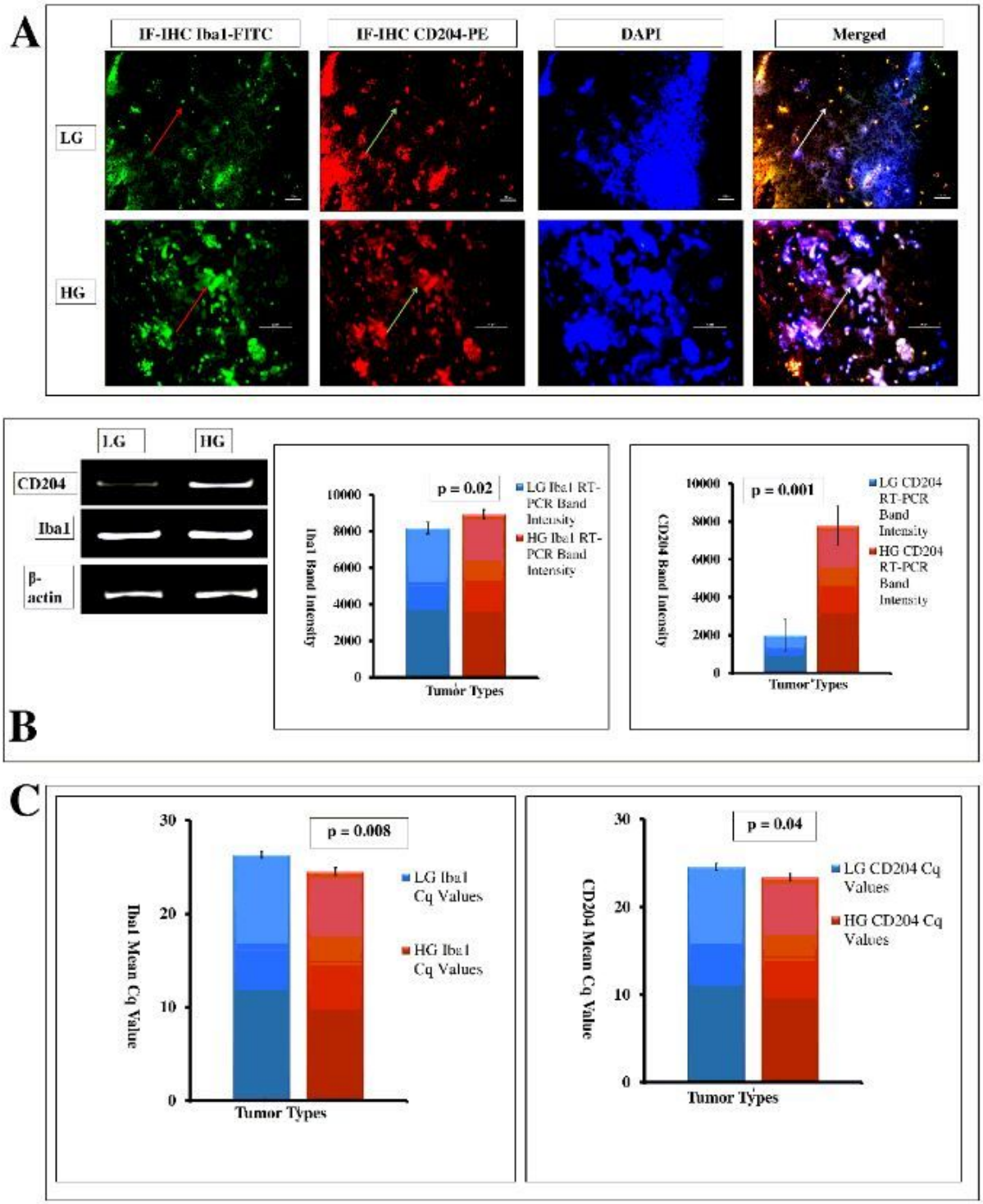

Figure 4

[A] Whole tissue IF-IHC with VEGF-PE and DAPI (400X, marked with green arrows) shows increased level of neoangiogenic expression in low grades (LG) rather high grades (HG). [B] ICC with isolated cells from tumor tissue also show increased level of VEGF expression (400X, marked with green arrows) in LG tumors than their HG counterparts. [C] cDNA gel band expression taking VEGF as target and β-actin as housekeeping, depicts higher level of capillary sprouting in LG tumors with p value of 0.02. [D] RNA expression by qRT-PCR suggests high Cq value in high grade tumors indicating their lower level of neoangiogenic ability than LG tumors (p=0.02). [E] MFI of VEGF in flowcytometry is concurrent with proliferation. In LG tumor, the expression is higher in whole tissue cell than the invaded counterparts; while in HG tumors, the level of angiogenic expression is higher in invaded cells than whole tissue cells ($p \geq 0.05$).

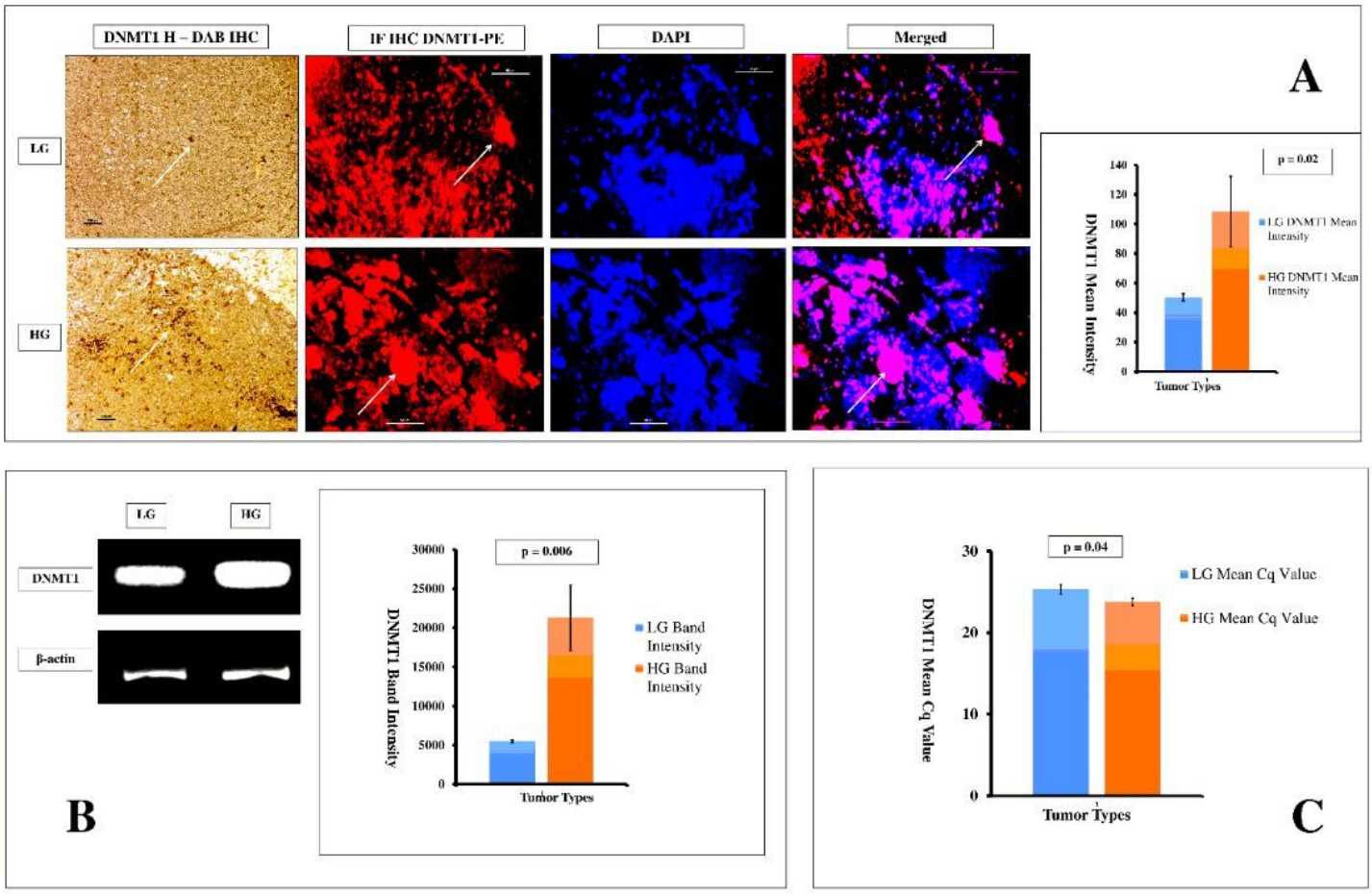

Figure 5

[A] Both the H-DAB IHC (100X) and IF-IHC with DNMT1 (with PE-conjugate at 400X) methylation marker in whole tumor tissue indicates higher expression of methylation in high grades (HG) than low types (LG). Plotted mean intensity expression from H-DAB IHC shows same result with p value of 0.02. [B] cDNA expression of RNA from both grades also show elevated expression of methylation induced by DNMT1 in high grade tumors (p=0.006). [C] Real time gene expression in qRT-PCR also denotes lower Cq level in HG DNMT1 expression in comparison to LG counterparts with significant p value of 0.04.

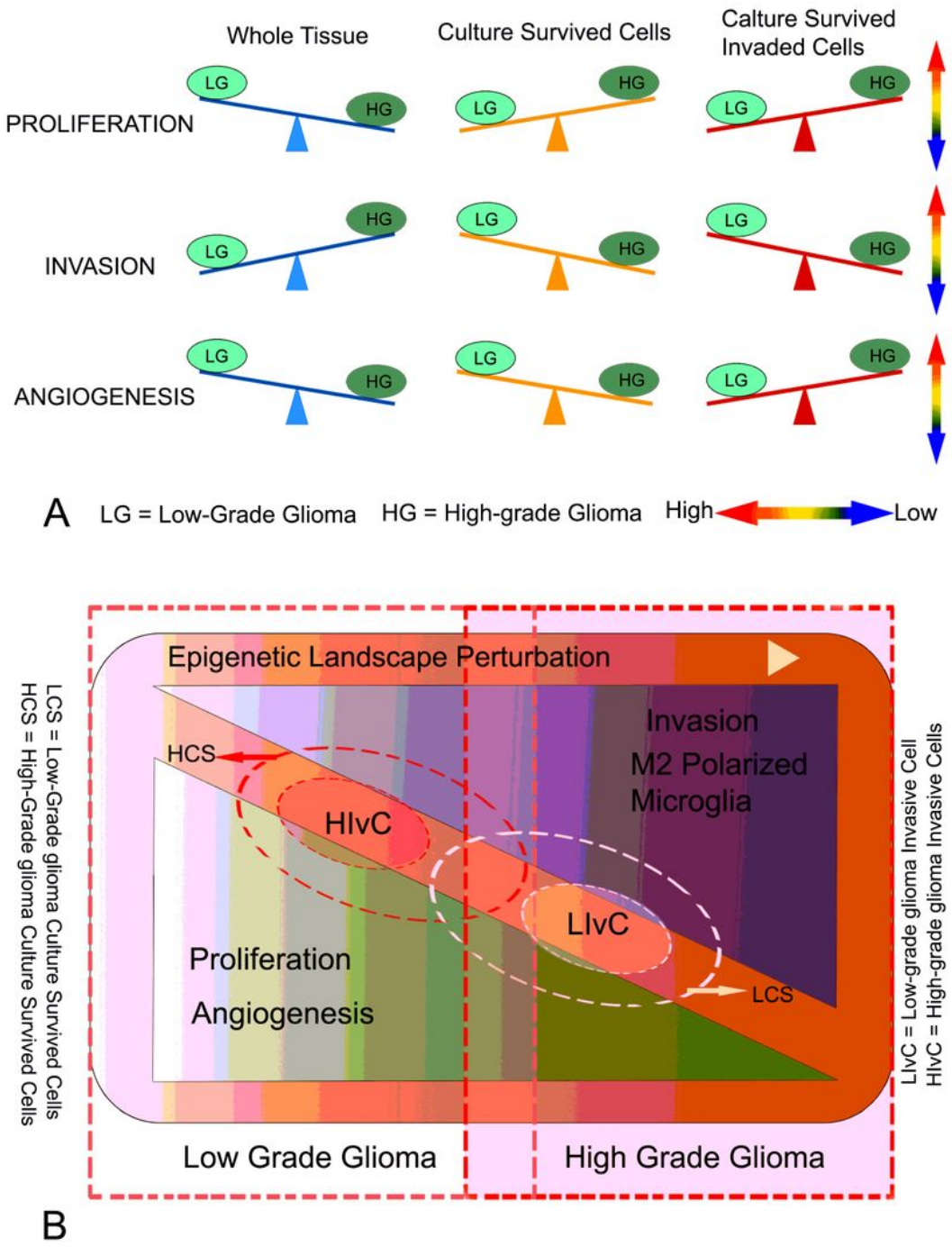

Figure 6

Glioma Tissue and its cellular variants showing behavioral differences among grades. Schematic representation of the facts: [A] the whole tissue in lower-grade glioma shows higher proliferative urges where high-grade is more inclined towards tissue degradation and invasion. This higher proliferative impulse in lower-grade glioma mass is supported by angiogenesis. But the culture survived cells and invading cells of high-grade are highly proliferative in comparison to their low-grade counterparts. This

has been generally supported by angiogenic factor for invading cells, but differs for culture survived cells. Therefore, differences exist among the cellular sub-sets and whole glioma tissue behavioral expression and a prominent dichotomy exists between proliferation coupled with angiogenesis and invasion, i.e., between ‘grow’ and ‘go’. [B] Overall data suggests that, on an increasingly perturbed epigenetic landscape lower grades of glioma tissue is more proliferative with all its cellular components by angiogenic funding, but higher grade glioma tissue is much damaging for the surroundings with high presence of M2 polarized GAM; and with notable contrast, the invading cells of high-grades are dangerously proliferative suggesting their intense drive to grow if entered in newer territories. [In this schematic diagram, the magnitude of inclinations and positions of the components are tentative showing their trends in general.]

Supplementary Files

This is a list of supplementary files associated with this preprint. Click to download.

- FigS1.tiff